Journal of Nature Studies 24(2): 1-13
Online ISSN: 2244-5226

SIMULATING DAILY RAINFALL FROM SEASONAL CLIMATE PROJECTIONS FOR CLIMATE RISK PLANNING

Azra May B. Kabiri[1*], Christian Alvin H. Buhat, Diane Carmeliza N. Cuaresma[1], Patricia Anne S. Delmendo[2], Jonathan B. Mamplata[1], Angelo E. Marasigan[1], Jerico E. Mendoza[2], Joy T. Santiago[2], John Kenneth B. Suarez[2], Alfredo Mahar Francisco A. Lagmay[2,3], and Genaro A. Cuaresma[1,3]

[1]Institute of Mathematical Sciences, College of Arts and Sciences, University of the Philippines Los Banos, 4031, Laguna, Philippines
[2]University of the Philippines Nationwide Operational Assessment of Hazards, Diliman, Quezon City, Philippines
[3]University of the Philippines Resilience Institute, Diliman, Quezon City, Philippines

*Corresponding author: abkabiri1@up.edu.ph

ABSTRACT – This study presents a stochastic method to decompose projected seasonal rainfall into daily rainfall using a first-order Markov chain for rainfall occurrence and a Gamma distribution for rainfall intensity. The model is applied to the National Capital Region (NCR) of the Philippines using historical daily rainfall data from 1970 to 2000 and seasonal climate projections from PAGASA (2018) under RCP 4.5 and RCP 8.5 scenarios. Transition probabilities are modeled as functions of seasonal rainfall totals, allowing daily rainfall sequences to be generated based on projected seasonal values. Simulation results reveal seasonal shifts in rainfall characteristics: the dry season (Dec-Jan-Feb) and early wet season (Mar-Apr-May) show increases in both wet-day frequency and intensity, while the wet season (Jun-Jul-Aug) and post-monsoon period (Sep-Oct-Nov) show decreases in both. While a single realization is shown for illustration, Z-scores are computed from 10,000 simulated realizations to assess the model's statistical consistency. While not intended for precise daily predictions, the model offers a useful tool for exploring plausible rainfall scenarios under climate change. The approach can support applications in flood risk assessment and adaptation planning. Future improvements may include higher-order Markov chains, alternative intensity distributions, and formal validation to enhance model accuracy and applicability across regions.

Keywords: climate change, decomposed seasonal rainfall, rainfall intensity, rainfall occurrence

INTRODUCTION

The Philippines, an archipelagic country in Southeast Asia, experiences monsoon rains and around 20 tropical cyclones or typhoons annually (DOST-PAGASA, 2011). These contribute to frequent flood-related disasters, resulting in loss of lives, property, and livelihoods (Hong et al., 2022; Villafuerte et al., 2015). As climate change intensifies, risks are expected to increase, making it important to develop

To cite this paper: Kabiri, A.M.B., Buhat, C.A.H., Cuaresma, D.C.N., Delmendo, P.A.S., Mamplata, J.B., Marasigan, A.E., Mendoza, J.E., Santiago, J.T., Suarez, J.K.B., Lagmay, A.M.F.A. & Cuaresma, G.A. 2025. Simulating Daily Rainfall from Seasonal Climate Projections for Climate Risk Planning. *Journal of Nature Studies, 24*(2), 1-13.

reliable rainfall projections to inform disaster prevention, adaptation, and mitigation planning (DOST-PAGASA & Manila Observatory Ateneo de Manila University, 2020; Hong et al., 2022; Villafuerte et al., 2020; Villafuerte et al., 2020; Worku et al., 2018; Yoo et al., 2016).

Daily rainfall projections are essential for a wide range of climate-sensitive applications that depend on the timing and intensity of rainfall events. For instance, flood simulations, drainage system design, and early warning systems depend on estimates of rainfall on specific days, particularly those that may trigger flooding. In agriculture, daily rainfall timing directly affects planting schedules, irrigation planning, and crop yields, especially for rainfed systems. Crops are often sensitive not only to the amount of rainfall but also to when it occurs during their growth stages (Rasool et al., 2024).

The Philippine Atmospheric, Geophysical and Astronomical Services Administration (PAGASA), the country's national weather and climate agency, regularly publishes assessments of the current and projected climate. In its 2011 report, PAGASA observed a non-statistically significant increase in the intensity and frequency of extreme rainfall events, and a similar trend in the number of strong tropical cyclones (with maximum sustained winds of 150 kph and above) based on data from 1951–2009 (DOST-PAGASA, 2011). A 2018 report highlighted spatial variability in rainfall trends (baseline 1971–2000), with Northern Luzon, Palawan, western Visayas, and parts of Mindanao experiencing decreasing annual rainfall, while the rest of the country saw increasing trends, particularly during the northeast monsoon season (DOST-PAGASA, 2018).

In the 2018 report, PAGASA provided seasonal (Dec–Jan–Feb, Mar–Apr–May, Jun–Jul–Aug, and Sep–Oct–Nov) rainfall projections per province to account for spatial variability. These projections were downscaled from global climate models under Representative Concentration Pathways (RCP) 4.5 and 8.5 for 2036–2065. RCP 4.5 is a stabilization scenario with intermediate greenhouse gas concentrations, while RCP 8.5 assumes high emissions (IPCC, 2014). Under RCP 8.5, rainfall in Mindanao could decrease by over 40%, while Luzon and western Visayas could see more than a 40% increase by mid-century. A more recent 2021 report provided projected climate extremes per province (baseline 1986–2005), showing a general decreasing trend in rainfall nationwide, with more localized extreme rainfall events (DOST-PAGASA & Manila Observatory Ateneo de Manila University, 2020). Other studies have similarly observed increasing rainfall during Dec–Jan–Feb and decreasing rainfall during Jun–Jul–Aug (Hong et al., 2022; Supari et al., 2020; Tangang et al., 2020; Villafuerte et al., 2015).

These seasonal projections, especially those from PAGASA, have been used in integrating scientific information into climate-sensitive development planning at local levels (DOST-PAGASA, 2018; DOST-PAGASA & Manila Observatory Ateneo de Manila University, 2020). However, their coarse temporal resolution limits their application in activities that require daily rainfall data, such as hydrologic modeling or flood simulations. Seasonal totals do not indicate which specific days will be rainy or how much rainfall will occur on each day. For decision-makers and modelers, it is crucial to identify not just the season, but the specific days when rainfall could reach flood-inducing levels. This information is vital for designing measures such as drainage systems, flood forecasting tools, and evacuation plans.

To bridge this gap, stochastic weather generators can be used to convert seasonal rainfall projections into daily rainfall realizations. Stochastic rainfall models account for the inherently random nature of rainfall occurrence and intensity. In a study from 2016, Yoo et al. used a first-order Markov chain to model monthly rainfall by estimating historical transition probabilities between wet and dry days and modeling rainfall intensity. They then incorporated climate projections to assess changes in daily rainfall characteristics not captured by shifts in wet-day frequency alone (Yoo et al., 2016).

Building on this, we apply a Markov chain-Gamma model to decompose PAGASA's 2018 seasonal rainfall projections into daily rainfall. We model daily rainfall occurrence using a two-state first-order Markov chain, with states representing rain or no rain, and transition probabilities capturing rainfall occurrence on a given day. After which, we use a Gamma distribution, which is suitable for positively skewed data, to model the rainfall intensity. We use historical daily rainfall data from the National Oceanic and Atmospheric Administration (NOAA) for the model. The focus of this study is the National Capital Region (NCR), an urban area highly vulnerable to flooding. We apply the model to PAGASA's lower bound, median, and upper bound seasonal rainfall projections for RCP 4.5 and 8.5 (Table B-1 in (DOST-PAGASA, 2018)). After developing the stochastic framework for disaggregating the seasonal rainfall projections as outlined above, we evaluate the performance of the model using Z-scores derived from historical observations and simulated rainfall. We apply the method to generate one possible daily rainfall time series under RCP 4.5 and RCP 8.5 scenarios for illustrative purposes, and we use the model parameters to derive projected daily rainfall characteristics.

While this study provides a useful method for decomposing seasonal rainfall projections into daily rainfall data, it also has several limitations. First, the model is based on past rainfall patterns and assumes that future rainfall will behave similarly. Thus, there may be rainfall patterns in the future that the model cannot predict. Second, although the Gamma distribution is good for modeling rainfall intensity, it may not fully capture very heavy rainfall events, like heavy monsoon rains or storm rains, that can cause major flooding. Third, the model does not consider changes in the timing or length of the rainy season, which could also shift in the future. Fourth, the model uses rainfall data that covers large areas, which may miss small-scale local differences. Lastly, we focused only on rainfall and did not include other factors such as temperature, humidity, or wind, which also affect agriculture and flood risk. We also only generated one possible version of a daily rainfall time series for each climate scenario. Since rainfall is random by nature, many possible outcomes exist, and a single version may not show the full range of possibilities. These limitations should be considered when interpreting the results and applying them in planning or decision-making.

MATERIALS AND METHODS

This section outlines the data sources, study area, and modeling framework used to disaggregate seasonal rainfall projections into daily rainfall estimates.

Study Area and Data Source

Daily rainfall data from 1 January 1970 to 31 December 2000 are collected from the Science Garden station in Quezon City, Philippines (Latitude: 14.65, Longitude: 121.05), as available from the National Oceanic and Atmospheric Administration (NOAA) (NOAA, n.d.).

We use the seasonal rainfall projections provided in Table B-1 DOST-PAGASA (2018) Observed and Projected Climate Change in the Philippines report for the National Capital Region (NCR), which includes lower bound, median, and upper bound estimates of seasonal changes (in both percentage and millimeters) for the years 2036–2065.

Modelling Daily Rainfall Occurrence

If $X_{t,k}$ is a random variable indicating rainfall occurrence on a day t in season k, where $k = 1,2,3,4$ corresponds to Dec–Jan–Feb, Mar–Apr–May, Jun–Jul–Aug, and Sep–Oct–Nov, respectively, we model $X_{t,k}$ as a two-state first-order Markov chain (see Yoo et al., 2016). A day is in state 1 (wet) if

rainfall exceeds 0 mm, and in state 0 (dry) otherwise. This results in four transition probabilities $p_{ij,k}$, where $i, j = 0,1$, denoting the probability of transitioning from state i on day $t-1$ to state j on day t, in season k. The transition probability $p_{10,2}$ denotes the likelihood that a day is dry (state 0) given that the previous day was wet (state 1), specifically within the March–April–May season.

Because a day can only be wet or dry, $p_{10,k} = 1 - p_{11,k}$ and $p_{01,k} = 1 - p_{00,k}$, we estimate only $p_{00,k}$ and $p_{11,k}$ using the linear regression models:

$$p_{00,k} = a_{0,k}S_k + b_{0,k}, \quad (1a)$$
$$p_{11,k} = a_{1,k}S_k + b_{1,k}. \quad (1b)$$

Here, S_k is the seasonal rainfall total, and $a_{i,k}$ and $b_{i,k}$ are regression parameters. The Ljung–Box autocorrelation test at lag 1 (5% significance level) confirms the presence of correlation between rainfall on consecutive days, supporting the use of the Markov model.

Modelling Daily Rainfall Intensity

If $Y_{t,k}$ is a random variable describing the rainfall intensity on day t in season k, conditional on $X_{t,k} = 1$, we assume $Y_{t,k}$ is independently and identically distributed (i.i.d.) and follows a Gamma distribution $Y_k \sim \Gamma(\alpha_k, \theta_k)$, where $\alpha_k > 0$ is the shape parameter and $\theta_k > 0$ is the scale parameter. The Gamma distribution is widely used to model skewed rainfall data (Chandler and Wheater, 2002; Martinez-Villalobos and Neelin, 2019).

We define the actual rainfall amount $R_{t,k}$ on day t in season k as:

$$R_{t,k} = \begin{cases} Y_{t,k}, & X_{t,k} = 1 \\ 0, & \text{otherwise} \end{cases}. \quad (2)$$

The expected total seasonal rainfall is given by:

$$\sum_{t=1}^{n_k} E[R_{t,k}] = n_k \pi_{1,k} E[Y_k], \quad (3)$$

where n_k is the number of days in the season k, $\pi_{1,k}$ denotes the stationary probability of being a wet day, and $E[Y_k]$ is the expected rainfall intensity.

Integration with Climate Projections

To incorporate climate change scenarios, we replace S_k in equations (1a) and (1b) with projected seasonal rainfall values from Table B-1 of (DOST-PAGASA, 2018). By doing so, we can compute new transition probabilities, ${p_{00,k}}'$ and ${p_{11,k}}'$, and the stationary probability ${\pi_{1,k}}'$. We rearrange equation (3) and solve for $E[Y_k]$ using the projected seasonal rainfall totals as a value for $\sum_{t=1}^{n_k} E[R_{t,k}]$. With the computed value for $E[Y_k]$, we can find the projected scale parameter ${\theta_k}'$ while retaining the shape parameter α_k.

Simulating Projected Daily Rainfall and Validation

We visualize one realization for lower, median, and upper bound situations for both RCP 4.5 and 8.5 using values for ${p_{00,k}}'$, ${p_{11,k}}'$ and ${\theta_k}'$. To evaluate the model's statistical consistency, we compute Z-scores from 10,000 simulated realizations.

All analyses, simulations, and visualizations are performed in Python 3.12.

RESULTS AND DISCUSSION

This section presents the results of the Markov chain-Gamma model used to generate daily rainfall estimates from seasonal climate projections for the National Capital Region (NCR) and discusses the implications of projected changes in daily rainfall patterns, particularly in the context of urban flood risk and climate prevention, mitigation, and adaptation strategies.

Description of Historical Data

Figure 1 shows the historical annual rainfall time series. The dataset exhibits a mean daily rainfall of 6.75 mm with a standard deviation of 18.41 mm. A few extreme values exceeding 250 mm, around 38 times the daily average, are present. Strong seasonality is evident: rainfall typically occurs from June to November, while the rest of the year is relatively dry, consistent with PAGASA's Climate Type 1 classification (DOST-PAGASA, 2011).

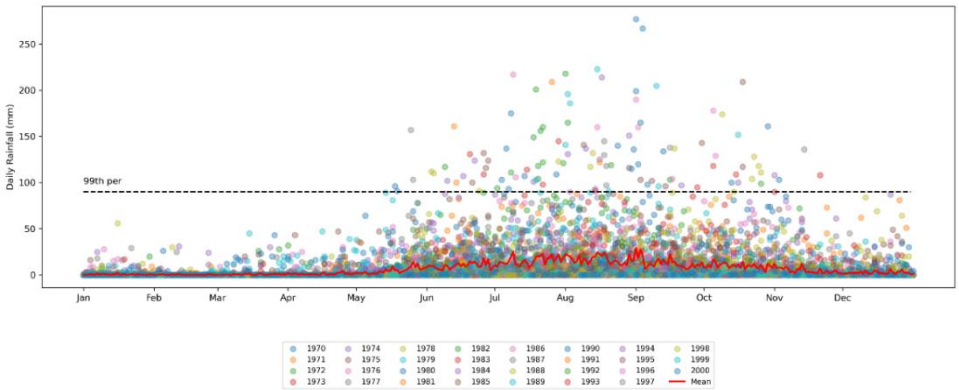

Figure 1. Observed total daily rainfall (in mm) from 1970 to 2000 in Science Garden station.

Table 1 summarizes key rainfall statistics per season. The Jun–Jul–Aug period is the wettest, with about 59 rainy days out of 92 and an average of approximately 14 mm of rain per day, equivalent to around 1,300 mm for the season. In contrast, the driest period is Dec–Jan–Feb, with only about 11 rainy days out of 90 and a seasonal total of roughly 100 mm. This seasonal difference highlights the strong monsoonal influence on NCR's climate.

The Jun-Jul-Aug season also exhibits the highest standard deviation of seasonal rainfall (492 mm), indicating high inter-annual variability. Moreover, this season also records the highest daily rainfall intensity values, with the 99th percentile reaching 105 mm. This shows the frequent occurrence of extreme rainfall events. Interestingly, Dec-Jan-Feb and Mar-Apr-May show extreme rainfall events, with the 99th percentile of daily rainfall exceeding 18 mm and 32 mm, respectively. All together, these results imply that extreme rainfall events can happen year-round and present challenges in making long-term forecasting and planning.

Table 1. Observed statistics of the historical daily rainfall from 1970 to 2000 in the Science Garden station.

Variable	Dec-Jan-Feb	Mar-Apr-May	Jun-Jul-Aug	Sep-Oct-Nov
Mean number of wet days	12.10	16.63	58.97	48.16
Std Dev of the number of wet days	7.70	8.36	12.45	12.76
Mean daily rainfall (in mm)	1.12	2.26	14.06	9.31
Std Dev of Daily Rainfall (in mm)	4.18	7.22	23.94	19.68
Mean of Seasonal Rainfall (in mm)	102.42	207.61	1293.10	847.42
Std Dev of Seasonal Rainfall (in mm)	105.24	152.29	491.74	341.81
99th Percentile of Daily Rainfall (in mm)	18.07	32.47	105.18	88.76

Projected Daily Rainfall

Historical Daily Rainfall Occurrence

The Markov chain model transition probabilities are estimated using linear regression on seasonal rainfall totals. Figure 2 shows observed seasonal rainfall totals and the fitted regression lines. The intercepts of dry-to-dry transition probabilities for Dec-Jan-Feb and Mar-Apr-May are close to 1 ($a_{0,1} = a_{0,2} = 0.94$), while Jun-Jul-Aug and Sep-Oct-Nov are moderate ($a_{0,3} = 0.54, a_{0,4} = 0.77$, respectively). As for the intercepts of wet-to-wet transition probabilities, $a_{1,1} = 0.20, a_{1,2} = 0.31, a_{1,3} = 0.66$ and $a_{1,4} = 0.52$. In all cases, the regression slopes are small, with a magnitude ≤ 0.001. Even with hypothetically extreme seasonal rainfall of 5000 mm, the transition probabilities would remain strictly between 0 and 1. With the exception of $p_{00,3}$, all fitted transition probabilities have R^2 values ranging from 20% to 50%.

Notably, all regression lines for dry-to-dry transition probabilities p_{00} are negatively sloping. This behavior is expected since the persistence of dry spells has a negative relationship with seasonal rainfall total. That is, as seasonal rainfall increases, the length of dry days decreases, which reduces the chance that a dry day is followed by another dry day. Dec–Jan–Feb and Mar–Apr–May exhibit the highest dry-to-dry transition probabilities, suggesting strong persistence of dry days during these seasons. On the other hand, all wet-to-wet transition probabilities p_{11} are positively sloping. This indicates that consecutive wet days are likely when the seasonal rainfall total is high. Jun–Jul–Aug, the wettest season as mentioned in the previous section, exhibits the highest wet-to-wet transition probability ($p_{11} = 0.66 + 0.00007S_3$).

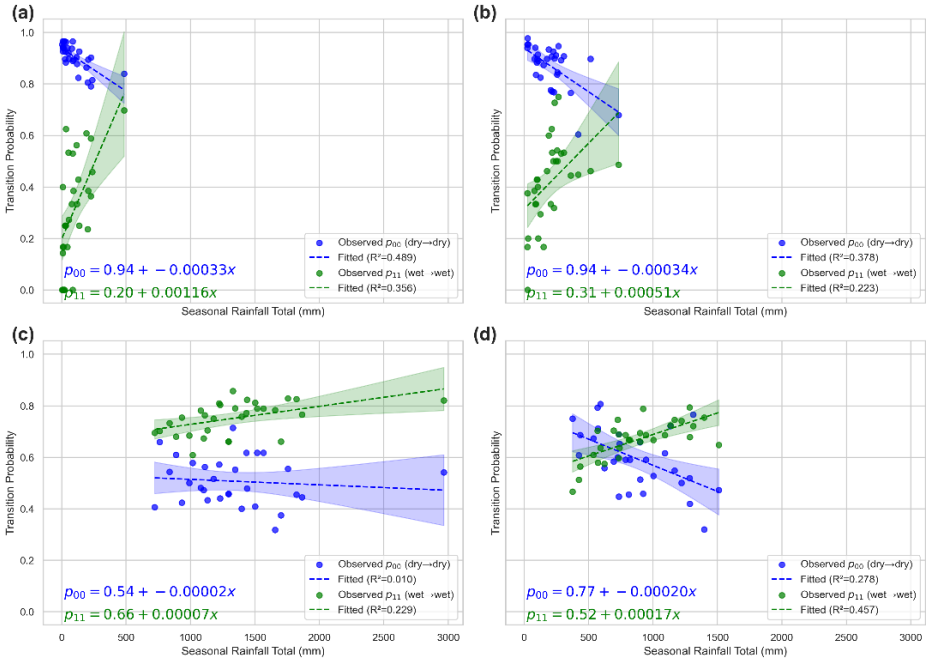

Figure 2. Observed regression relationship between seasonal rainfall totals and daily transition probabilities p_{00} (dry-to-dry) and p_{11} (wet-to-wet) for (a) Dec-Jan-Feb, (b) Mar-Apr-May, (c) Jun-Jul-Aug, and (d) Sep-Oct-Nov.

Historical daily rainfall intensity

The rainfall intensity on wet days is modelled using a Gamma distribution. Figure 3 shows the histogram of rainfall intensity and the fitted Gamma distributions together with parameter estimates and some error statistics. Results show that the fitted Gamma distributions follow the historical rainfall histograms, as evidenced by the low root mean square error (RMSE) and mean absolute error (MAE) values.

The shape parameter α_k is similar across seasons (0.73-0.82), which indicates that the overall shape of rainfall distribution is consistent all year round. On the other hand, the scale parameter θ_k is higher for Jun–Jul–Aug (28.14) and Sep–Oct–Nov (24.08), which indicates that the average intensity of rainfall during these seasons is higher. Because $\alpha_k > \theta_k$ for all k, the distribution is right-skewed—capturing the observed pattern of many low-rainfall days and a few extreme rainfall events.

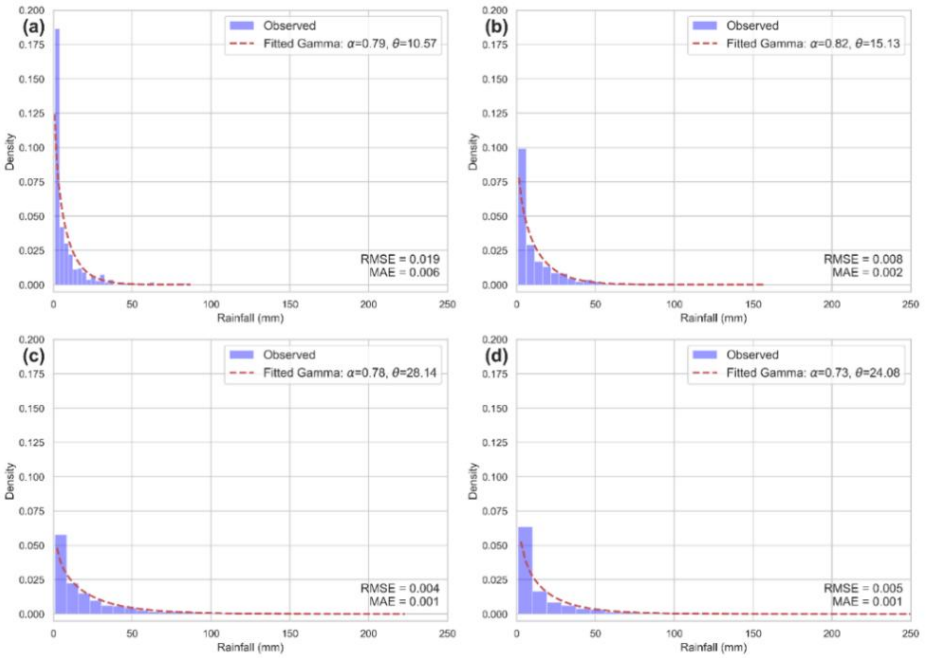

Figure 3. Daily rainfall intensity fitted with a Gamma distribution for (a) Dec-Jan-Feb, (b) Mar-Apr-May, (c) Jun-Jul-Aug, and (d) Sep-Oct-Nov.

Projected Daily Rainfall Daily

Table 2 presents the comparison of transition probabilities and scale parameters decomposed from PAGASA's 2018 seasonal projections under RCP 4.5 and RCP 8.5 scenarios (Table 2). These results allow for a deeper understanding of how rainfall occurrence and intensity may evolve in the future across seasons.

In Dec-Jan-Feb, there is an increase in the probability of wet-to-wet days accompanied by a rise in rainfall intensity. Results are similar in Mar-Apr-May, though changes are less pronounced. These patterns imply intensification of wet conditions during these seasons. In contrast, Jun-Jul-Aug and Sept-Oct-Nov exhibit an increase in the probability of dry-to-dry days and a decrease in rainfall intensity. These shifts indicate a drier season, with fewer wet days and reduced rainfall amounts. These changes are illustrated in Figure 4, which shows the Z-score of median projected rainfall in relation to the historical values. Dec-Jan-Feb shows the highest positive Z-score, which implies wetter conditions. In Mar-Apr-May, the Z-score remains positive but very close to zero, indicating almost no change from the historical value. The latter seasons show negative Z-scores, implying drier conditions. These align with PAGASA's projected changes, supporting the model's consistency. Overall, these seasonal changes have important implications for water resource planning, agriculture, and disaster preparedness, as they point to possible increased flood risks early in the year and drought risks in the latter months. Using the updated parameters in Table 2, a sample daily rainfall time series is simulated (Figure 5). Due to the model's stochastic nature, other outcomes are also possible.

Table 2. Projected daily rainfall parameters for years 2035 to 2065 per season.

	Historical	RCP 4.5			RCP 8.5			Interpretation
		Lower bound	Median	Upper bound	Lower bound	Median	Upper bound	
$p'_{00,1}$	0.90620	0.9026	0.8962	0.8827	0.9016	0.8926	0.8834	Increased number of wet days and intensity of rainfall
$p'_{11,1}$	0.31880	0.3214	0.3437	0.3909	0.3250	0.3564	0.3884	
θ_1'	10.57	12.2750	13.3007	14.8545	12.4557	13.7922	14.7882	
$p'_{00,2}$	0.8694	0.8717	0.8675	0.8557	0.8770	0.8688	0.8587	Slight increase in wet days and intensity of rainfall
$p'_{11,2}$	0.41588	0.4155	0.4218	0.4395	0.4075	0.4197	0.4349	
θ_2'	15.13	14.6635	15.0340	15.9304	14.1533	14.9147	15.7160	
$p'_{00,3}$	0.2814	0.5157	0.5129	0.5105	0.5146	0.5119	0.5085	Decreased number of wet days and intensity of rainfall
$p'_{11,3}$	0.75051	0.7221	0.7313	0.7393	0.7256	0.7346	0.7459	
θ_3'	28.14	20.2096	22.7566	24.9065	21.1943	23.6511	26.6663	
$p'_{00,4}$	0.6005	0.6345	0.6270	0.6059	0.6301	0.6118	0.5872	Decreased number of wet days and intensity of rainfall
$p'_{11,4}$	0.6641	0.6341	0.6403	0.6577	0.6378	0.6528	0.6731	
θ_4'	24.08	20.3548	21.0762	22.9664	20.7799	22.4589	24.5088	

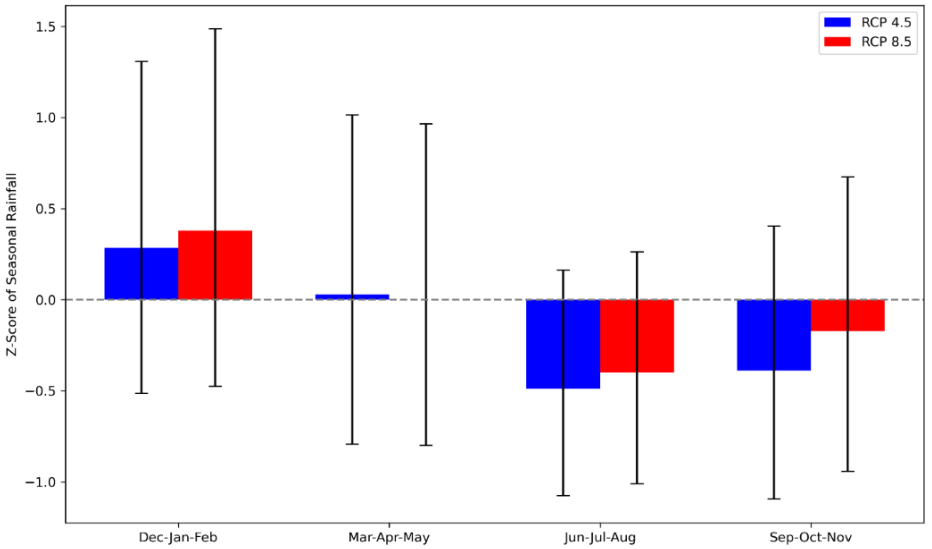

Figure 4. Z-scores of median projected seasonal rainfall under RCP 4.5 and RCP 8.5 (10,000 simulations).

CONCLUSION

This study applied a first-order Markov chain and a Gamma distribution to statistically model the occurrence and intensity of daily rainfall, respectively. The main objective was to decompose projected seasonal rainfall into daily rainfall, using historical data and seasonal climate projections from PAGASA under RCP 4.5 and RCP 8.5 scenarios. By incorporating projected seasonal totals into the Markov chain–Gamma framework, the model produced plausible daily rainfall sequences, offering a way to explore future rainfall scenarios at a daily scale. While only a single realization was generated for illustration, 10,000 simulations were performed per scenario to compute Z-scores, which assess how well the simulated rainfall statistics align with expected seasonal behaviors.

The model does not aim to predict the exact occurrence or intensity of rainfall on specific days. Rather, it provides a probabilistic understanding of how rainfall characteristics may shift under climate change—such as changes in the number of wet days or the distribution of rainfall intensity—which can be inferred from changes in model parameters. The results indicate that the first half of the year (Dec-Jan-Feb and Mar-Apr-May) may experience an increase in the number of wet days and rainfall intensity, while the second half (Jun-Jul-Aug and Sep-Oct-Nov) may see fewer wet days and less intense rainfall. This information can be valuable for water resource planning, flood risk assessment, and climate adaptation strategies.

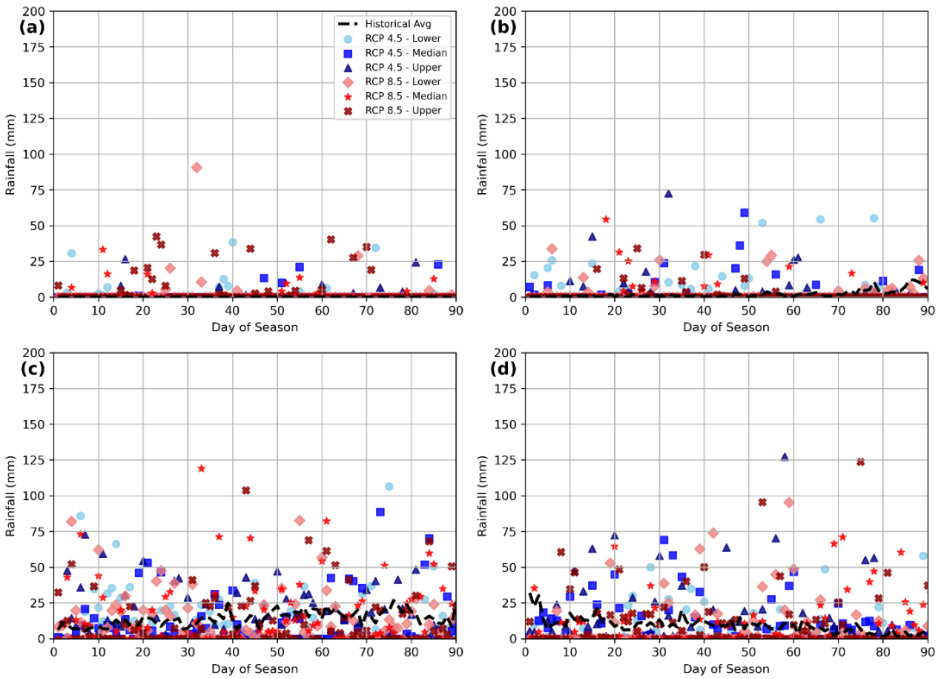

Figure 5. Simulated daily rainfall under RCP 4.5 and RCP 8.5 scenarios for (a) Dec-Jan-Feb, (b) Mar-Apr-May, (c) Jun-Jul-Aug and (d) Sep-Oct-Nov.

Nonetheless, several limitations should be noted. The model assumes stationarity within each season and was applied to data from a single station, which may limit its generalizability across regions. The Gamma distribution was selected for computational efficiency but not formally tested for goodness-of-fit. Nevertheless, model performance was assessed using root mean square error (RMSE) and mean absolute error (MAE) between simulated and historical seasonal rainfall totals. Additionally, the model treats seasons independently and may underestimate long-term variability, particularly in seasonal aggregates.

Future work may explore higher-order Markov chains to account for more complex temporal dependencies in rainfall occurrence. New or alternative probability distributions could be evaluated to better capture rainfall extremes. Machine learning techniques may also offer promising avenues for long-term rainfall modeling and projection. Ultimately, improving the model's accuracy and applicability will require formal validation using proven statistical tests and application across diverse climatic settings.

ACKNOWLEDGEMENT

This study was conducted as part of the University of the Philippines Resilience Institute project 'Formulation of the Quezon City Drainage Master Plan (QC DMP)'.

DATA AVAILABILITY STATEMENT

No new data were generated in this study. The code used for data processing and analysis is available from the corresponding author upon reasonable request.

STATEMENT OF AUTHORSHIP

A.M.B. Kabiri, C.A.H. Buhat, D.C.N. Cuaresma, J.B. Mamplata, A.E. Marasigan, A.M.F.A. Lagmay, and G.A. Cuaresma conceptualized the study. A.M.B. Kabiri, C.A.H. Buhat, J.B. Mamplata, and A.E. Marasigan developed the model and methodology. A.M.B. Kabiri and D.C.N. Cuaresma performed the numerical simulations and conducted the analysis. P.A.S. Delmendo, J.E. Mendoza, J.T. Santiago, and J.K.B. Suarez handled project administration. A.M.F.A. Lagmay and G.A. Cuaresma provided supervision and academic guidance. All authors participated in the writing of the manuscript.

REFERENCES

Chandler, R. E. and Wheater, H. S. (2002). Analysis of rainfall variability using generalized linear models: A case study from the west of Ireland. Water Resources Research, 38(10), 10-1-10–11. https://doi.org/10.1029/2001WR000906

Chowdhury, A. F. M. K., Lockart, N., Willgoose, G., Kuczera, G., Kiem, A. S., and Parana Manage, N. (2017). Development and evaluation of a stochastic daily rainfall model with long-term variability. Hydrology and Earth System Sciences, 21(12), 6541–6558. https://doi.org/10.5194/hess-21-6541-2017

DOST-PAGASA. (2011). Climate change in the Philippines. https://www.pagasa.dost.gov.ph/information/climate-change-in-the-philippines

DOST-PAGASA. (2018). Observed climate trends and projected climate change in the Philippines. https://www.dost.gov.ph/knowledge-resources/downloads/file/689-observed-climate-trends-and-projected-climate-change-in-the-philippines.html

DOST-PAGASA and Manila Observatory Ateneo de Manila University. (2020). Philippine climate extremes report 2020. Philippine Atmospheric, Geophysical and Astronomical Services Administration.

Hong, J., Agustin, W., Yoon, S., and Park, J.-S. (2022). Changes of extreme precipitation in the Philippines, projected from the CMIP6 multi-model ensemble. Weather and Climate Extremes, 37, 100480. https://doi.org/10.1016/j.wace.2022.100480

IPCC. (2014). Climate change 2014: Synthesis report. Contribution of working groups I, II and III to the fifth assessment report of the Intergovernmental Panel on Climate Change.

Martinez-Villalobos, C., and Neelin, J. D. (2019). Why do precipitation intensities tend to follow Gamma distributions? Journal of the Atmospheric Sciences, 76(11), 3611–3631. https://doi.org/10.1175/JAS-D-18-0343.1

NOAA. (n.d.). Global historical climatology network - Daily (GHCN-Daily), Version 3. https://www.ncei.noaa.gov/access/search/data-search/dailysummaries?fbclid=IwAR0lC4cX75Mx9aLwMAofNjWKWIqIaTcytC0A8i5y8DVY0BN7llRdKbG-WcY

Rasool, G., Anjum, M. N., Kim, D. Y., Azam, M., Hussain, F., Afzal, A., Maeng, S. J., and Min, K. C. (2024). Projecting Climate Change Impact on Precipitation Patterns during Different Growth Stages of Rainfed Wheat Crop in the Pothwar Plateau, Pakistan. Climate, 12(8), 110. https://doi.org/10.3390/cli12080110

Supari, Tangang, F., Juneng, L., Cruz, F., Chung, J. X., Ngai, S. T., Salimun, E., Mohd, M. S. F., Santisirisomboon, J., Singhruck, P., PhanVan, T., Ngo-Duc, T., Narisma, G., Aldrian, E., Gunawan, D., and Sopaheluwakan, A. (2020). Multi-model projections of precipitation extremes in Southeast Asia based on CORDEX-Southeast Asia simulations. Environmental Research, 184, 109350. https://doi.org/10.1016/j.envres.2020.109350

Tangang, F., Chung, J. X., Juneng, L., Supari, Salimun, E., Ngai, S. T., Jamaluddin, A. F., Mohd, M. S. F., Cruz, F., Narisma, G., Santisirisomboon, J., Ngo-Duc, T., Van Tan, P., Singhruck, P., Gunawan, D., Aldrian, E., Sopaheluwakan, A., Grigory, N., Remedio, A. R. C., … Kumar, P. (2020). Projected future changes in rainfall in Southeast Asia based on CORDEX–SEA multi-model simulations. Climate Dynamics, 55(5–6), 1247–1267. https://doi.org/10.1007/s00382-020-05322-2

Villafuerte, M., Lambrento, J. C., Ison, C. M., Vicente, A. A., de Guzman, R., and Juanillo, E. (2021). ClimDatPh: an online platform for Philippine climate data acquisition. Philippine Journal of Science, 150(1), 53-66.

Villafuerte, M. Q., Macadam, I., Daron, J., Katzfey, J., Cinco, T. A., Ares, E. D., and Jones, R. G. (2020). Projected changes in rainfall and temperature over the Philippines from multiple dynamical downscaling models. International Journal of Climatology, 40(3), 1784–1804.

https://doi.org/10.1002/joc.6301

Villafuerte, M. Q., Matsumoto, J., and Kubota, H. (2015). Changes in extreme rainfall in the Philippines (1911-2010) linked to global mean temperature and ENSO. International Journal of Climatology, 35(8), 2033–2044. https://doi.org/10.1002/joc.4105

Worku, G., Teferi, E., Bantider, A., Dile, Y. T., and Taye, M. T. (2018). Evaluation of regional climate models performance in simulating rainfall climatology of Jemma sub-basin, Upper Blue Nile Basin, Ethiopia. Dynamics of Atmospheres and Oceans, 83, 53–63. https://doi.org/10.1016/j.dynatmoce.2018.06.002

Yoo, C., Lee, J., and Ro, Y. (2016). Markov chain decomposition of monthly rainfall into daily rainfall: Evaluation of climate change impact. Advances in Meteorology, 2016, 1–10. https://doi.org/10.1155/2016/7957490